Synthesis of cross-linking chitosan-PVA composite hydrogel and adsorption of Cu(II) ions

Qingping Song, Jiangang Gao, Ying Lin, Ze Zhang and Yixin Xiang

ABSTRACT

A cross-linked chitosan-PVA spherical hydrogel (CSH) was synthesized and its structure was characterized by Fourier transform infrared spectroscopy (FTIR), scanning electron microscopy (SEM) and X-ray diffraction (XRD). The physical and chemical properties of CSH, such as acid resistance and swelling, were determined. Finally, Cu(II) ion removal by the CSH was investigated, and the effects of experimental parameters, including pH, adsorption time, and regeneration performance were examined. Results revealed that CSH has outstanding stability in strong acid solution, thus extending the useful pH range as an adsorbent material. The maximum capacity of CSH for Cu(II) was obtained to be 62.1 mg/g at 25 °C for 24 h. The adsorption process was best described by a pseudo-second-order kinetic model, while isotherm modeling revealed that the Langmuir equation better described the adsorption of Cu(II) on CSH. Moreover, the loaded CSH can be easily regenerated by the HCl-washing method and reused repeatedly for Cu(II) adsorption for up to five cycles.

Key words | adsorption, chitosan, cross-linking, heavy metals, hydrogel, PVA

Qingping Song (corresponding author)
Jiangang Gao
Ying Lin
Ze Zhang
Yixin Xiang
School of Biochemical and Engineering,
Anhui Polytechnic University,
Anhui,
China
E-mail: *adsqp@163.com*

HIGHLIGHTS

- A novel cross-linked CS/PVA hydrogel (CSH) was synthesized by a two-step method.
- The physical and chemical properties of CSH, such as acid resistance and swelling, were determined.
- The CSH has outstanding stability in strong acid solution, thus extending the useful pH range as an adsorbent material.
- Unlike traditional powder adsorbents, the spherical CSH beads, with a mean diameter of 3 mm, are easily separated after adsorption.
- The loaded CSH can be easily regenerated by the HCl-washing method and reused repeatedly for Cu(II) adsorption.

GRAPHICAL ABSTRACT

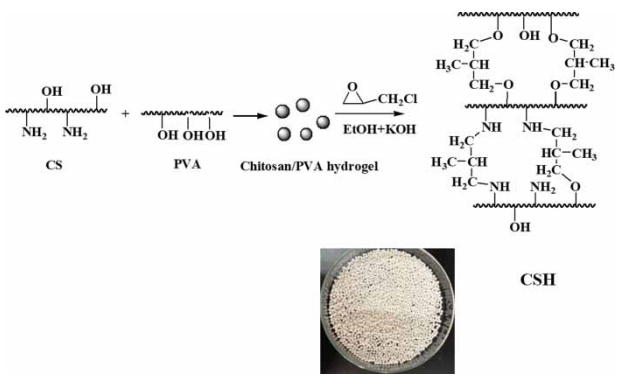

doi: 10.2166/wst.2020.204

INTRODUCTION

Water pollution by heavy metals is becoming a severe global issue due to the toxicity, non-degradability and cumulative nature of heavy metals through the food chain. Copper is often detected in industrial wastewaters, which originates from mining activities, metal plating, smelting, battery manufacture, tanneries, petroleum refining, paint and pigment manufacture, and so on (Karaer & Kaya 2017). The industrial waste effluents contain a large amount of copper pollutants, which are harmful to human health and ecological systems. The main methods for removing Cu(II) from an aqueous environment include ion exchange, chemical precipitation, membrane filtration and adsorption, etc (Shalla *et al.* 2019), and adsorption has been found to be the best technology due to its high efficiency, eco-friendliness, low operating cost and easy operation (Agarwal & Singh 2017). Numerous methods have been made by various researchers to develop cheaper and effective adsorbents to remove Cu(II) ions from waste water (Ayoub *et al.* 2013; Sahebjamee *et al.* 2019). Recently, bioadsorbents have been receiving increasing attention due to their nontoxic, biodegradable and natural availability (Muya *et al.* 2016). Among these, chitosan (CS) is an abundant biopolymer obtained by deacetylation of chitin and has a good adsorption ability for heavy metal ions because of its good metal-binding capacities, biodegradability and low toxicity (Salehi *et al.* 2016). However, pure chitosan materials also have some obvious disadvantages, such as low mechanical strength, poor acid resistance and difficult recovery (Peng *et al.* 2014). To overcome these disadvantages, considerable efforts have been made by chemical cross-linking or blending CS with other polymers, such as polyvinyl alcohol (PVA), cellulose and polyacrylamide (Zhang *et al.* 2016). Among the various polymers, PVA is one of materials used for interesting blends with chitosan due to its low cost, good mechanical properties and nontoxic nature. Chitosan blended with PVA has been reported to have good mechanical and chemical properties because of the formation of intermolecular hydrogen bonds (Karaer & Kaya 2017; Abdolmaleki *et al.* 2018). Also, it is necessary for composite hydrogel to enhance acid resistance ability through the cross-linking reaction.

In the past years, some researchers have employed various cross-linking agents (such as epichlorohydrin, glyoxal, glutaraldehyde and tripolyphosphate) to eliminate solubility concerns and improve the mechanical properties of chitosan composites (Salehi *et al.* 2016).

In the present work, a cross-linked chitosan-PVA spherical hydrogel (CSH) with good adsorption capability and low cost was synthesized by a two step method. First, chitosan/PVA composite spherical hydrogel was prepared via the phase inversion method. Then, the obtained composite hydrogel was crosslinked with epichlorohydrin in basic condition. The prepared CSH was characterized by Fourier transform infrared spectroscopy (FTIR), scanning electron microscopy (SEM) and X-ray diffraction (XRD) to identify the structures and morphology. Unlike traditional powder adsorbents, the CSH, with a mean diameter of 3 mm, is easily separated and regenerated in acid solution. In addition, the CSH adsorbent was completely insoluble in strong acid solution because of the formation of a three-dimensional network structure in the cross-linking reaction, which benefits industrial wastewater treatment. Finally, the adsorbent was used for adsorption of Cu(II) from aqueous solutions. The initial pH value, adsorption time and regeneration ability were investigated in the experiment. The adsorption experimental data were studied based on isotherm and kinetic models.

MATERIALS AND METHODS

Materials

Chitosan (93% deacetylated) was obtained from Sinopharm Chemical Reagent Co., Ltd (Shanghai, China). PVA (1788) was supplied by Macklin, Shanghai China. $CuSO_4{\cdot}5H_2O$, KOH, HNO_3, HCl and epichlorohydrin were of analytical grade and were obtained from Shanghai Chemical Co, China. All the solutions were prepared with distilled water.

Synthesis of cross-linking chitosan-PVA spherical hydrogel (CSH)

2.0 g chitosan was dissolved in 48 mL of 2% acetic acid until a clear solution was obtained. Meanwhile, 2.0 g PVA was dissolved in 18 mL distilled water by heating the solution at 90 °C under strong stirring for 30 min. Next, the above two solutions were mixed together for 3 h by magnetic stirring. The resultant homogeneous solution was left in the beaker to sufficiently free the air bubbles. After that, the solution was added dropwise to a 5% NaOH solution through a 16G syringe needle (1.15 mm inner diameter) and the formed hydrogel was immersed in a 5% NaOH solution to neutralize the excess acid for 2 h. Then, the chitosan/PVA spherical hydrogel was filtered and washed repeatedly with distilled water until all alkali was removed.

The prepared chitosan/PVA hydrogel was cross-linked with epichlorohydrin (4 mL) in 100 mL ethanol solvent containing 0.1 M potassium hydroxide. After reaction for 3 hours at 50 °C, the cross-linked hydrogel was filtered and washed with ethanol several times, and then freeze-dried for 24 h to obtain CSH. The average diameter of the freeze-dried CSH is about 3.0 mm and the preparation process is illustrated in Figure 1.

Acid resistance and swelling ratio test

To determine the degree of acid resistance (AR%) and swelling ratio (SR%), 200 mg dried CSH (Wi, initial mass) was dispersed in three kinds of 100 mL acidic aqueous solutions, respectively. The mixed solution was stirred at room temperature. After 24 h, the CSH was filtered and weighed (*Ws*, swollen mass). In the sequence, CSH was dried at 105 °C until mass stabilization and the final weight was recorded (W_f, final mass). AR % and SR% were calculated using Equations (1) and (2), respectively (Perumal *et al.* 2019).

$$\mathrm{AR}(\%) = \frac{W_f}{Wi} * 100\% \tag{1}$$

$$\mathrm{SR}(\%) = \frac{Ws - W_i}{Wi} * 100\% \tag{2}$$

Characterization of the chitosan-PVA spherical hydrogel

FTIR spectra of the samples were measured using a Fourier transform infrared spectrometer, Model EQUINOX55 (Bruker). A Hitachi S-4800 (Japan) scanning electron microscopic (VP-SEM) was used to examine the microstructure of chitosan and CSH. X-ray diffraction patterns of chitosan, PVA and CSH were measured using an X-ray diffractometer (D8-Advance, Bruker).

Batch Cu(II) removal experiments

Batch adsorption experiments were carried out to evaluate adsorption capacities of CSH and all adsorption experiments were carried out at 25 °C. $CuSO_4{\cdot}5H_2O$ was used as sources of Cu(II). Typically, 100 mg of CSH was added into a 50 mL solution of known Cu(II) concentrations and stirred at a fixed speed (150 rpm) with a thermostatic stirrer. The initial pH value was adjusted by 0.1 M HCl or 0.1 M NaOH solutions using a Model PHS-25 pH-meter (Shanghai Leici, China). At a given time, the CSH was filtrated from the solutions and the concentration of Cu(II) remaining in the solution was determined by atomic absorption spectrophotometer (TAS900, Beijing Purkinje). The adsorption capacity of adsorbent (q) was calculated according to the following equation:

$$q = \frac{v(C_i - C_f)}{m} \tag{3}$$

where q is the metal adsorption capacity (mg/g), C_i is the initial concentration of Cu(II) (mg/L), C_f is the final concentration of Cu(II) (mg/L), V is the volume of the solution (L), and m is the weight of CSH added into the flask.

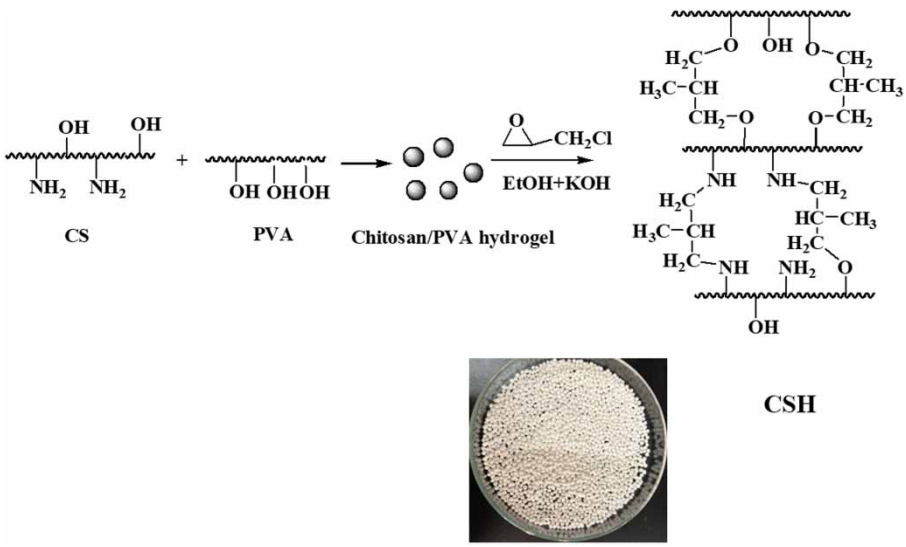

Figure 1 | Preparation scheme of CSH adsorbent.

To determine the kinetics performances, 100 mg of CSH was added to 50 mL of Cu(II) solution (100 mg/L or 200 mg/L). The mixture was then stirred, samples were filtered at different time intervals and the filtrate solution was analyzed. Equilibrium adsorption isotherm experiments were conducted over a range of initial Cu(II) concentrations from 50 to 200 mg/L. 100 mg of CSH was added into 50 mL of the solutions. The mixtures were stirred at 25 °C for 24 h. After adsorption, the solution was filtered and the final concentration of Cu(II) was determined.

Adsorption–desorption study

After the Cu(II) was adsorbed, the CSH was added into 100 mL 0.1 mol/L HCl for 3 h to ensure the desorption of Cu(II) from the adsorbent. To use the adsorbent in the next cycle, it was washed several times with distilled water. Then, the treated CSH was applied in the recycled adsorption study. The adsorption/desorption measurements were repeated five times.

RESULTS AND DISCUSSION

Characterization of the CSH

To investigate the interaction between the chitosan and PVA molecules, chitosan, PVA, and CSH were characterized by FTIR. FTIR spectra of chitosan, PVA and CSH before and after Cu(II) adsorption are shown in Figure 2. In the spectrum of chitosan, the major bands can be assigned as follows: 3,423 cm^{-1} (–OH and $–NH_2$ stretching vibrations), 2,883 cm^{-1} (–CH stretching vibration), 1,639 cm^{-1} (amide I), 1,600 cm^{-1} ($–NH_2$ bending vibration), 1,325 cm^{-1} (stretching vibration of C–N), 1,153 cm – 1 (bridge-O-stretch), 1,035 and 1,078 cm^{-1} (primary and secondary stretching vibration of C–OH) (Song *et al.* 2017; Yu *et al.* 2017). For PVA, the broad characteristic peak appeared at 3,427 cm^{-1} relating to the stretching -O-H group. Peaks at around 2,978 cm^{-1} and at 1,402 cm^{-1} corresponded to the C-H stretching and $-CH_2-$ bending from alkyl groups, respectively. The strong peak at 1,635 cm^{-1} indicates the presence of acetate groups of PVA. This is related to the partial (87% – 89%) hydrolyzation of the PVA. In addition, the peak at 1,093 cm^{-1} is attributed to the C–OH stretching of PVA (Jamnongkan *et al.* 2014). Compared with the spectra of chitosan and PVA, the wide peak at 3,433 cm^{-1} of CSH corresponding to the stretching vibration of the $–NH_2$ group and –OH group shifted to a higher frequency. The strong band at 1,600 cm^{-1} assigned to the free amino group disappeared and shifted to 1,639 cm^{-1} (C = O stretching vibration of PVA and N – H bending vibration of chitosan), indicating $–NH_2$ groups take part in the crosslinking reaction. Furthermore, the peaks of primary and second C – OH stretching vibration were also overlapped and shifted to 1,082 cm^{-1}. All of these results confirmed that intermolecular hydrogen bonding and crosslinking reaction formed among $–NH_2$ and -OH groups in CSH. After adsorption of Cu(II), significant changes in the FTIR spectrum were found at the wavenumbers of 3,407 cm^{-1}, 1,635 cm^{-1} and 1,111 cm^{-1}. Therefore, it can be concluded that the adsorption mainly occurred at the $-NH_2$ and -OH groups of CSH.

The morphology of chitosan (a1, a2) and CSH (b1, b2) was assessed through SEM. As is depicted in Figure 3, the pure chitosan appears to have a smooth and homogeneous surface. On the contrary, the surface of CSH shows a

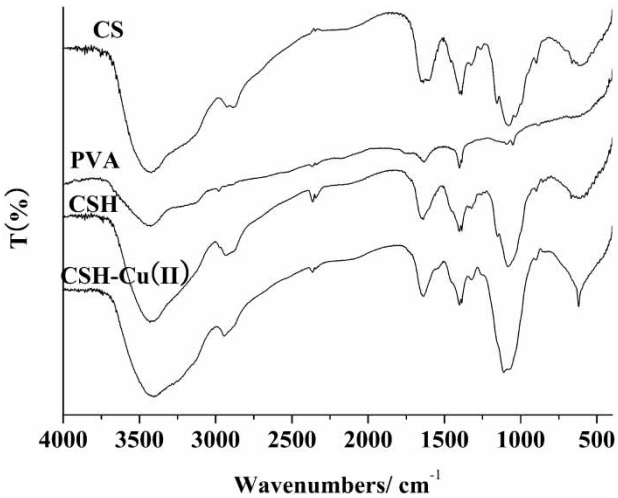

Figure 2 | FTIR spectra of chitosan (CS), PVA and CSH before and after Cu(II) adsorption.

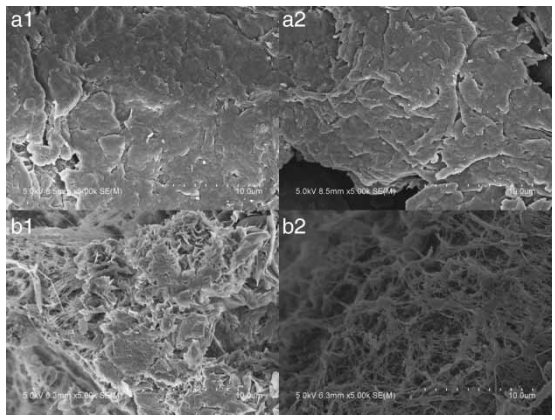

Figure 3 | SEM images of the chitosan (a1, a2) and CSH adsorbent (b1, b2).

highly porous structure, these structures will provide a convenient diffusion channel benefit to adsorption of Cu(II). The porous structure of CSH was probably caused by the presence of extensive hydrogen bonding between the functional groups of the two polymers and chemical crosslinking processes (Hu *et al.* 2018).

Figure 4 shows the XRD patterns for chitosan, PVA and CSH. It can be seen that there are some differences in peak heights between them. Chitosan reveals a significant crystalline peak near 20°, and the characteristic peak of PVA was at around 19.5° of 2θ (Kalantari & Afifi 2018). However, CSH has a relatively characteristic peak that was significantly weakest. It is well known that the XRD peak is related to the size of crystallite, a weaker peak usually results from small crystallites (Song *et al.* 2011). Hence, the crystalline structure of CSH was destroyed due to forming a new interpenetrating network structure by the chemical crosslinking reaction (Ahmad *et al.* 2017).

Acid resistance analysis

Acid resistance is an important property for adsorbent materials used in water treatment. Because most Cu(II) ion-containing industrial wastewater is acidic and pure chitosan and PVA dissolve in acid conditions, the ability of the CSH to resist acid was investigated. Here, the structural stability of the CSH was evaluated by directly observing the weight loss in the acid solutions after 24 h. The results are presented in Table 1. Dissolution testing has shown that CSH is completely insoluble in acidic solutions and there is no change in the mass loss. These findings demonstrated that the cross-linking significantly improved the chemical and structural stability of the hydrogel in our experimental conditions. This is very significant for the application of the adsorbents in real engineering and adsorbent regeneration. In contrast, the acid resistance of uncross-linked chitosan/PVA adsorbent was tested in the experiment. It was found that uncross-linked chitosan/PVA hydrogel was completely dissolved in an acid solution after about 5 min. Therefore, the cross-linking reaction was successful in our study. The swelling degree of the composite was also investigated. As can be seen, the swelling ratios of CSH varied from 433–663%.

Table 1 | The acid resistance and swelling ratio of CSH

	0.1 M HCl	0.2 M HCl	0.1 M HNO_3	0.2 M HNO_3	0.2 M HOAc	0.5 M HOAc
Acid resistance (%)	102.2	99.5	105.1	104.8	99.7	100.1
Swelling ratio (%)	663.7	633.3	644.7	614.7	433.8	458.1

Effect of pH

The effect of initial solution pH on Cu(II) removal by CSH is shown in Figure 5. As indicated in Figure 5, the pH of the aqueous solution was clearly an important parameter that controlled the adsorption process. Within the range of pH values, which varied from 2.0 to 3.0, the adsorption capacity significantly increased from 13.3 to 56.7 mg/g. With further increase of pH (3.0–5.5), the adsorption capacity of Cu(II) gradually reached the maximum of 62.1 mg/g at pH 5.5. At pH values higher than 5.5, the adsorption capacity of CSH decreased to 59.5 mg/g. Therefore, pH 5.5 was selected as the optimal value for Cu(II) adsorption on the CSH. This can be explained by the fact that at low pH the amino groups on CSH can easily protonate, inducing an electrostatic repulsion of Cu(II) (Yang *et al.* 2019).

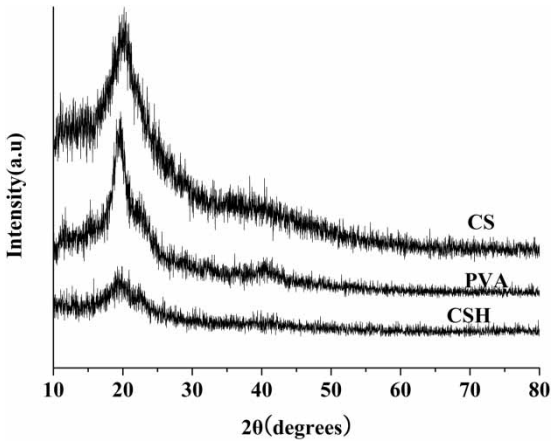

Figure 4 | XRD patterns of chitosan, PVA, and CSH adsorbent.

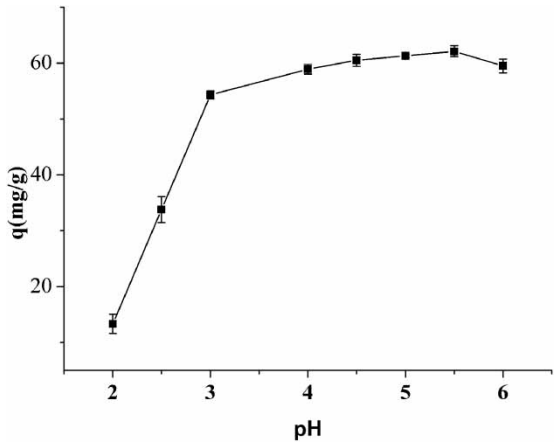

Figure 5 | Effect of pH on the removal of Cu(II) using CSH (Cu(II): 200 mg/L; dosage, 2.0 g/L; contact time, 24 h; temp, 25 °C).

Effect of contact time and kinetic modeling

Adsorption time is an important parameter because it can reflect the adsorption kinetics of an adsorbent. The effect of contact time on the adsorption of CSH for Cu(II) was investigated at different initial solute concentrations and the results are shown in Figure 6. It was found that the absorbed amount of Cu(II) increased with increasing Cu(II) concentration. This might be because, at higher concentrations, the driving force for ion migration between the aqueous phase and solid phase enhanced (Zhang *et al.* 2018). In addition, the rates of adsorption of Cu(II) on CSH were seen to increase markedly during the first 480 min and gradually approach the limiting adsorption after 1,440 min (24 h). The explanation may be that a large number of free adsorption sites on the surface were void and that Cu(II) easily interacted with these sites during the initial stage. With increasing time, the remaining vacant sites are not easily occupied due to the reduction of the adsorption sites (Peng *et al.* 2014). Then, the adsorption rate slows down and gradually reaches equilibrium.

In order to investigate the adsorption mechanisms, the adsorption experimental data were fitted using the nonlinear form of the pseudo-first-order (Equation (4)) and the pseudo-second-order equations (Equation (5)) (Zhang *et al.* 2016).

$$q_t = q_e(1 - e^{-k1t}) \tag{4}$$

$$q_t = \frac{k_2 q_e^2 t}{1 + k_2 q_e t} \tag{5}$$

where q_e and q_t (mg/g) are the adsorption capacities of Cu(II) ions adsorbed onto CSH at equilibrium and at time t, respectively. k_1 (min^{-1}) and k_2 (g/mg·min) are adsorption rate constants of the pseudo-first-order and pseudo-second-order, respectively.

Then, the two kinetic models were applied to fit the experimental data, respectively. The nonlinear fitting results are also shown in Figure 6 and their parameters are all listed in Table 2. Based on the analysis of correlation coefficients (R^2), the pseudo second-order model gives an R^2 mean value (0.995) higher than that of the pseudo-first-order model (0.986). The adsorption behavior of Cu(II) on CSH obeyed the pseudo-second-order kinetic model, suggesting the adsorption of Cu(II) is controlled mainly by the chemisorption mechanism (Pu *et al.* 2018).

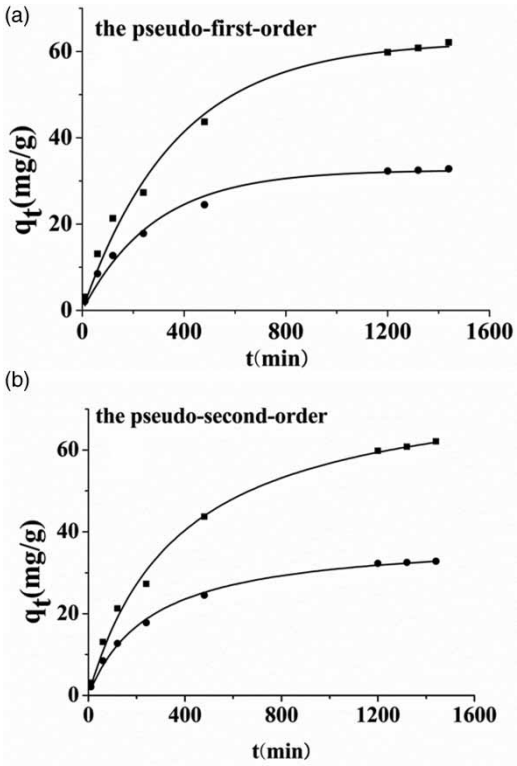

Figure 6 | Kinetic adsorption results of Cu(II) on the CSH, (a) Cu(II) fitted with pseudo-first order models; (b) Cu(II) fitted with pseudo-second order models (pH = 5.5; dosage, 2.0 g/L; temp, 25 °C).

Desorption and regeneration analysis

Recycle studies were performed to explore the sustainability and cost effectiveness of the CSH. Most adsorbents are in the form of powder to increase the contact area of the adsorbent and the solution, which clearly leads to difficulty in collecting the adsorbent after sorption (Yu *et al.* 2017). In contrast, spherical CSH can easily desorb the bound metals under acid conditions and be collected after adsorption. In addition, during the adsorption and desorption process, the CSH adsorbent showed good mechanical stability.

Table 2 | Parameters of kinetic models of Cu(II) adsorption onto CSH

		Ion concentration (mg/L)	
Kinetic model	**Model parameter**	**200 mg/L**	**100 mg/L**
Pseudo-first-order model	q_e-exp (mg/g)	62.1	32.8
	q_e-cal (mg/g)	62.4	32.5
	k_1 (min^{-1})	0.00273	0.00352
	R^2	0.987	0.984
Pseudo-second-order model	k_2 (10^4 g/mg.min)	3.467	1.008
	q_e-cal (mg/g)	77.8	38.6
	R^2	0.993	0.996

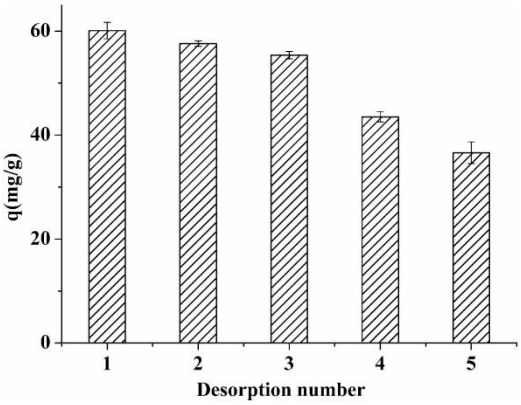

Figure 7 | Adsorption capacity of CSH adsorbent for Cu(II) during cyclic experiments (initial concentration, 200 mg/L; dosage, 2.0 g/L; at pH 5.5; desorption time, 180 min; temp, 25 °C).

In the desorption experiment (see Figure 7), five adsorption-desorption cycles were conducted, and 0.1 M HCl solution was found to be effective to desorb Cu(II) from the adsorbent. The adsorption capacity of Cu(II) on CSH decreased slowly with increasing cycle numbers over three cycles, and at the end of five regeneration cycles, the sorption capacity maintained 60% of the initial value. The results indicated that CSH could be used repeatedly in Cu(II) adsorption.

Adsorption isotherms

The adsorption isotherm model describes the interaction of adsorbate with adsorbents and is important for predicting the adsorption performance of the adsorbent. Two of the most commonly used isotherm theories have been adopted in this work, namely Langmuir and Freundlich (Ahmed & Hameed 2019). The Langmuir isotherm model is assumed to have affinity for monolayer adsorption. Whereas the Freundlich isotherm adsorption model considered that multilayer adsorption occurs on heterogeneous surfaces (Homayonfard *et al.* 2018). The nonlinear forms of the Langmuir and Freundlich isotherms are given as follows:

$$\text{Langmuir isotherm model: } q_e = \frac{q_m K_L C_e}{1 + K_L C_e} \quad (6)$$

$$\text{Freundlich isotherm model: } q_e = K_F C_e^{1/n} \quad (7)$$

where C_e (mg/L) is the equilibrium concentration of residual ions in the solution and q_m is the maximum amount of adsorption (mg/g), K_L (L/mg) is the constant related to the affinity of the adsorbent binding site, K_F ((mg/g) (L/mg)$^{1/n}$) and n are the Freundlich constants related to the adsorption capacity and adsorption intensity, respectively.

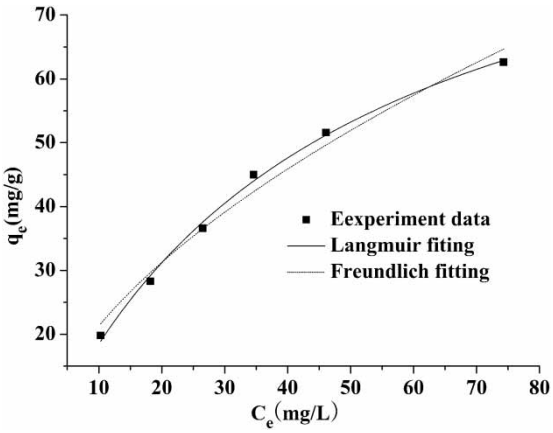

Figure 8 | Adsorption isotherm data of Cu(II) onto CSH (initial pH, 5.5; Initial Cu(II) concentration ranging from 50 to 200 mg/L; dosage, 2.0 g/L; adsorption time, 24 h; temp, 25 °C).

Table 3 | Non-linear isothermal parameters for the adsorption of Cu(II) onto CSH

Langmuir			Freundlich		
q_m (mg/g)	K_L	R^2	K_F	n	R^2
100.5	0.02251	0.996	5.9462	1.805	0.979

Figure 8 displays the non-linear plots of fitting models. The parameters calculated are listed in Table 3. It is clear that the adsorption isotherm results can be well described by the Langmuir model ($R^2 > 0.99$), with q_m on CSH being 100.5 mg/g. Hence, the adsorption behavior of Cu(II) on CSH suggested a monomolecular layer adsorption (Hu *et al.* 2018).

CONCLUSIONS

In the present study, cross-linked chitosan-PVA spherical hydrogel (CSH) was prepared and characterized. The adsorption parameters were evaluated by using the batch adsorption method, and adsorption equilibrium was obtained in 24 h at pH 5.5 with adsorption capacity of 62.1 mg/g. The kinetics of the experimental data were fitted with the pseudo-second-order model and the Langmuir model fitted the adsorption data better. Adsorption–desorption studies showed that CSH was completely regenerated for up to five cycles using 0.01 M HCl with the loss of adsorption capacity. In summary, a low-cost CSH exhibited good adsorption ability, excellent anti-acid property in strong acid and good regeneration ability. Thus, the composite hydrogels can potentially be used for the removal of Cu(II) from wastewater.

ACKNOWLEDGEMENTS

This work was financially supported by the Natural Science Foundation of Anhui Province (No. 1908085QB63).

REFERENCES

Abdolmaleki, A. Y., Zilouei, H., Khorasani, S. N. & Zargoosh, K. 2018 Adsorption of tetracycline from water using glutaraldehyde-crosslinked electrospun nanofibers of chitosan/poly (vinyl alcohol). *Water Science and Technology* **77** (5), 1324–1335.

Agarwal, M. & Singh, K. 2017 Heavy metal removal from wastewater using various adsorbents: a review. *Journal of Water Reuse and Desalination* **7** (4), 387–419.

Ahmed, M. J. & Hameed, B. H. 2019 Insights into the isotherm and kinetic models for the coadsorption of pharmaceuticals in the absence and presence of metal ions: a review. *Journal of Environmental Management* **252**, 109617.

Ahmad, M., Manzoor, K., Chaudhuri, R. R. & Ikram, S. 2017 Thiocarbohydrazide cross-linked oxidized chitosan and Poly(vinyl alcohol): a green framework as efficient Cu(II), Pb(II), and Hg(II) adsorbent. *Journal of Chemical & Engineering Data* **62**, 2044–2055.

Ayoub, A., Venditti, R. A., Pawlak, J. J., Salam, A. & Hubbe, M. A. 2013 Novel hemicellulose–chitosan biosorbent for water desalination and heavy metal removal. *ACS Sustainable Chemistry & Engineering* **1** (9), 1102–1109.

Homayonfard, A., Miralinaghi, M., Shirazi, R. H. S. M. & Moniri, E. 2018 Efficient removal of cadmium (II) ions from aqueous solution by $CoFe_2O_4$/chitosan and $NiFe_2O_4$/chitosan composites as adsorbents. *Water Science and Technology* **78** (11), 2297–2307.

Hu, T., Liu, Q., Gao, T., Dong, K., Wei, G. & Yao, J. 2018 Facile preparation of tannic acid–poly (vinyl alcohol)/sodium alginate hydrogel beads for methylene blue removal from simulated solution. *ACS Omega* **3** (7), 7523–7531.

Jamnongkan, T., Kantarot, K., Niemtang, K., Pansila, P. P. & Wattanakornsiri, A. 2014 Kinetics and mechanism of adsorptive removal of copper from aqueous solution with poly (vinyl alcohol) hydrogel. *Transactions of Nonferrous Metals Society of China* **24** (10), 3386–3393.

Kalantari, K. & Afifi, A. M. 2018 Novel chitosan/polyvinyl alcohol/talc composite for adsorption of heavy metals and dyes from aqueous solution. *Separation Science and Technology* **53** (16), 2527–2535.

Karaer, H. & Kaya, İ. 2017 Synthesis, characterization and using at the copper adsorption of chitosan/polyvinyl alcohol magnetic composite. *Journal of Molecular Liquids* **230**, 152–162.

Muya, F. N., Sunday, C. E., Baker, P. & Iwuoha, E. 2016 Environmental remediation of heavy metal ions from aqueous solution through hydrogel adsorption: a critical review. *Water Science and Technology* **73** (5), 983–992.

Peng, S., Meng, H., Ouyang, Y. & Chang, J. 2014 Nanoporous magnetic cellulose–chitosan composite microspheres: preparation, characterization, and application for Cu(II) adsorption. *Industrial & Engineering Chemistry Research* **53** (6), 2106–2113.

Perumal, S., Atchudan, R., Yoon, D. H., Joo, J. & Cheong, I. W. 2019 Spherical chitosan/gelatin hydrogel particles for removal of multiple heavy metal ions from wastewater. *Industrial & Engineering Chemistry Research* **58** (23), 9900–9907.

Pu, S., Hou, Y., Yan, C., Ma, H., Huang, H., Shi, Q. & Chu, W. 2018 *In situ* coprecipitation formed highly water-dispersible magnetic chitosan nanopowder for removal of heavy metals and its adsorption mechanism. *ACS Sustainable Chemistry & Engineering* **6** (12), 16754–16765.

Sahebjamee, N., Soltanieh, M., Mousavi, S. M. & Heydarinasab, A. 2019 Removal of Cu^{2+}, Cd^{2+} and Ni^{2+} ions from aqueous solution using a novel chitosan/polyvinyl alcohol adsorptive membrane. *Carbohydrate Polymers* **210**, 264–273.

Salehi, E., Daraei, P. & Shamsabadi, A. A. 2016 A review on chitosan-based adsorptive membranes. *Carbohydrate Polymers* **152**, 419–432.

Shalla, A. H., Yaseen, Z., Bhat, M. A., Rangreez, T. A. & Maswal, M. 2019 Recent review for removal of metal ions by hydrogels. *Separation Science and Technology* **54** (1), 89–100.

Song, Q., Zhang, Z., Gao, J. & Ding, C. 2011 Synthesis and property studies of N-carboxymethyl chitosan. *Journal of Applied Polymer Science* **119** (6), 3282–3285.

Song, Q., Wang, C., Gao, J. & Ding, Y. 2017 Synthesis and characterization of N-succinyl-O-carboxymethyl chitosan for Pb(II) ions adsorption. *Desalination and Water Treatment* **71**, 359–368.

Yang, K., Wang, G., Liu, F., Wang, X. & Chen, X. 2019 Removal of multiple heavy metal ions using a macromolecule chelating flocculant xanthated chitosan. *Water Science and Technology* **79** (12), 2289–2297.

Yu, P., Wang, H. Q., Bao, R. Y., Liu, Z., Yang, W., Xie, B. H. & Yang, M. B. 2017 Self-assembled sponge-like chitosan/reduced graphene oxide/montmorillonite composite hydrogels without cross-linking of chitosan for effective Cr (VI) sorption. *ACS Sustainable Chemistry & Engineering* **5** (2), 1557–1566.

Zhang, L., Zeng, Y. & Cheng, Z. 2016 Removal of heavy metal ions using chitosan and modified chitosan: a review. *Journal of Molecular Liquids* **214**, 175–191.

Zhang, Y., Lin, S., Qiao, J., Kołodyńska, D., Ju, Y., Zhang, M. & Dionysiou, D. D. 2018 Malic acid-enhanced chitosan hydrogel beads (mCHBs) for the removal of Cr(VI) and Cu(II) from aqueous solution. *Chemical Engineering Journal* **353**, 225–236.

First received 11 February 2020; accepted in revised form 16 April 2020. Available online 28 April 2020